Numerical Simulation Applied in Identification of Roof Bed Separation for Mining Thick Coal Seam Under Nappe Structure

Numerical Simulation Applied in Identification of Roof Bed Separation for Mining Thick Coal Seam Under Nappe Structure

Herong Gui [1], Rongjie Hu [3] Zhiyong Kang [2] Huili Qiu [1,4] Jun Li [1,4]

[1] Suzhou University, National Engineering Research Center of Coal Mine Water Hazard Control, Suzhou, Anhui, China
[2] No.115 Prospecting Institute of Coal Geology of Shanxi Province, Shanxi, China
[3] Wanbei Coal-Electricity Group Co. Ltd, Suzhou, Anhui, 234000, China
[4] Anhui University of Science & Technology, School of Earth and Engineering, Huainan, Anhui, China

hrgui@163.com

Abstract. In China coalmines, economic losses and human casualties inflicted by roof bed separation water have been acutely severe in recent years. This article takes the engineering case, mining thick coal seam under nappe, in Xinji No. 1 Coalmine in Huainan mining field. Given the low tensile strength of lower roof bed under large mining heights, numerical simulation is applied to No. 1307 fully mechanized top-coal caving (FMTC) working face by coupling elastoplastic finite element model (FEM) in rock mechanics with "no-tension analysis" (NTA) to map out, in the roof bed, pattern of stress distribution and the maximum heights of caving zone (37m) and of water-conductive fractured zone (98.5m), quantitatively delineating the location of bed separation. Specifically, bed separation F is the closest to the water-conductive fractured zone (by merely 1.93m) and of a maximum width of 6.4m, flagging a major threat to mining safety. These results are further corroborated by exploratory drills. Outcomes can be of reference to other coal-mining countries when identifying bed separation and treating related water hazards during mining under complex geological conditions.

1. Introduction

There are over 30 types of water hazards in China coalmines, including, among others, pore water, fissure water, and karst water [1-2]. In recent years, the number of water accidents caused by bed separation water has been climbing, inflicting severe economic losses and human casualties, and invited close examination by mining enterprises and mining experts. Between September 2009 and March 2010, four incidents of bed separation water burst struck No. 1121 working face of Hongliu Coalmine, Ningxia Yuanyang Lake Mining field, maximum water burst reaching 3,000 m3/h. The working face was buried under water and production was halted, incurring huge economic losses. On January 30, 2015, a major bed separation water accident hit No. 866-1 working face in Zhuxianzhuang Coalmine, Anhui Huaibei Mining field, known as the 1/30 Accident in which 7 miners were killed.

In coal seam, the roof bed comprises strata of varying thicknesses and hardness. During mining, the thick hard strata and the underlying soft strata would be displaced, creating interspace as upper thick hard strata hang over the subsided lower soft strata subside [3-4], known as bed separation. Underground water flows into the interspace and forms bed separation water. As backstoping

proceeds, suspension in the upper thick hard strata could be overstretched and rupture, which generates enormous impact instantly slamming bed separation water to explode [5-7] or sometimes causing rock burst. At Haizi Coalmine, Anhui Huaibei Mining field, mining at No. 745 working face was under thick igneous rock. On May 21, 2005, the igneous rock strata ruptured abruptly. Bed separation water between the strata and coal seam was smacked into the working face and took 5 lives. The rupture also caused rock burst with twice the energy in 1-magnitude earthquake, smashing underground tunnels and facilities [8-9].

Researches are abundant trying to understand the formation of bed separation in coalmines, so as identification techniques [10-13]. Kuznetsov et al. [14-15] observed in field experiments that bed separations tend to form on the sliding face with soft contact and that the formation process is closely related to the stress condition and strength of the sliding face. With these findings, Kuznetsov et al. put forward a method to forecast the developmental stage of bed separation based on geological structure and rock physical mechanics. Qian et al. [16-18] maintained that the thick hard strata play controlling role in the roof rock movement, thus proposing the key strata theory that lend scientific support for bed separation identification and treatment of bed separation water. Zhang et al. [19-20] took angle from structural mechanics and analyzed the mechanical conditions by way of rock physics central to the formation of bed separation after mining, on the basis of which to map potential locations of bed separations and calculated maximum separation width.

The roof rock over coal seam have a stratified structure, looking like rock plates of varying thicknesses overlying one another. Therefore, it is viable to abstract the deformation of the rock plates composition to that of multiple composition boards under mining disturbance. Given that each compoboard has a deflection different from the others, separation would form between compoboards that can be determined by calculation [21-22]. In recent years, numerical simulation in rock mechanics has played eminent roles in identifying bed separation [23-25]. Su et al. [26-27] worked with RFPA (rock failure process analysis code) software to simulate quantitatively non-linear deformation and failure in rock mass, the results from which were used to capture the characteristics of bed separation in mining and controlling factors.

Sedimentary structure of coal seam is complicated by alternating occurrences of normal succession (young to old from top down) or reversed succession (old to young from top down). For reversed succession, there are two scenarios. In one scenario, the strata are reversed under the horizontal tectonic stress. In the other, old strata are pushed over younger ones by nappe tectonic forces. In Xijin No. 1 Coalmine, Anhui Huainan Mining field of North China, nappe tectonic forces superimposed the lower Proterozoic gneiss strata above Permian coal seam. Production in the same coalmine focuses on the 13-1# thick coal seam, under the imminent threat from bed separation water. This article, incorporating characteristics of roof rock movement and deformation when mining thick coal seam under nappe structure, introduces application of numerical simulation by coupling elastoplastic finite element model (FEM) in rock mechanics with “no-tension analysis” (NTA), with considerations of stress distribution and deformation pattern, to quantitatively locate bed separation and calculate maximum separation width.

2. Sampling and testing

Huainan mining field is in the northeast of the North China coal-bearing area, with Laorencang normal fault on the south border and Minglongshan reverse fault on the north, Guchang normal fault to the east and Kouziji normal fault to the west (Figure 1). The mining field is 180km long from west to east and 15-25km wide from north to south, covering roughly 3,200 km^2. Early in the Indosinian-Yanshanian orogenic period, massive nappe tectonic movement took place in Huainan mining field. The resulting Fufeng thrust fault pushed the lower Proterozoic gneiss strata over Permian coal seam. The target area, Xinjin No. 1 Coalmine, is southern in Huainan mining field, where the majority working faces (such as No. 1305, No. 1307, etc.) are under the nappe structure formed by lower Proterozoic gneiss strata. The nappe structure spreads west to east by 1,000-1240m by a depth of 0-156m.

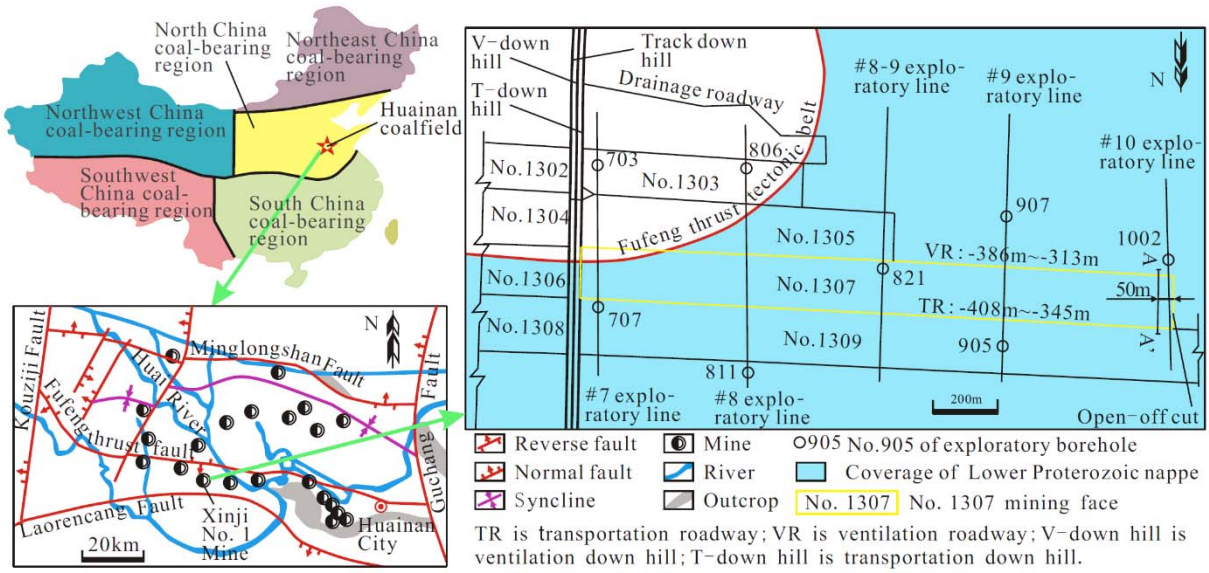

Figure 1. Map of target area and exploratory drills

Samples of rock core, from coal seam, roof rock, and floor rock, were obtained through exploratory drills (Figure 1) and immediately pre-treated in wrapping paper and sealed in wax. The samples were later reshaped into cylinder or cube according to the testing requirements. Samples by 5cm diameter and 10cm height were tested for uniaxial compressive strength; 5cm diameter and 2.5cm height for tensile strength; 5cm side-length cubes for shear test. Mechanical parameters, including compressive strength, tensile strength, shear strength, were tested on WEM screen-mounted hydraulic universal machine. For each type of test, 3 specimens from each stratum of rock and coal were processed and tested in parallel. The average of the 3 tests is shown in Table 1.

3. Calculation and discussion

3.1 Working face overview

The 1307 fully mechanized top-coal caving (FMTC) working face in Xinji No.1 Coalmine had a ventilation roadway (VR) elevation of -386m to -313m and a transportation roadway (TR) elevation of -408m to -345m, with ground elevation of +26m, strike length of 1350m, and slope width of 150m. The main mining seam was marked as 13-1#, with a thickness of 6m to 10m (average 8m) and an inclination angle of 6° to 10° (average 8°). Mining applied fully mechanized top-coal caving (FMTC) technique and the roof rock was managed by allowing full caving.

Table 1 shows that the roof rock over coal seam 13-1# is composed of mainly Permian coal-bearing strata and lower Proterozoic gneiss. Specifically, Permian coal-bearing strata (①~⑦), thickness of 86.95m, are fine sandstone, siltstone, mudstone, etc.; further up are the mélange strata in nappe tectonic belt (⑧), thickness between 0.7m and 17.4m or average of 13.5m, which are formed of napping clastic rocks and coal dust compacted by overlying roof strata; further up are lower Proterozoic gneiss (⑨~○,11), thickness of 118.37m, made of granitic gneiss and hornblende gneiss; above lower Proterozoic gneiss are Cainozoic Quaternary loose bed (○,12), average thickness of 183.93, consisted of clay, sandy clay, and fine silt.

Table 1. Testing results of physico-mechanical indicators of mid-layer strata in roof rock and coal seam

Period	Number of Strata	Avg. thickness $\overline{M}$ /m	Lithology	Density γ/t.m^{-3}	Compressive strength R_c/Mpa	Tensile strength R_t/Mpa	Cohesion C/Mpa	Internal friction angle φ/°	Elasticity modulus E×10^4 /Mpa	Poisson's ratio μ
Q	⑫	183.93	loose beds	2.000						
Pt_3	⑪	38.37	hornblende gneiss	2.600	73.69	1.49	8.04	46.26	5.43	0.21
	⑩	41.31	granitic gneiss	2.510	98.24	3.38	11.98	45.16	5.97	0.25
	⑨	38.69	hornblende gneiss	2.500	72.53	1.52	7.72	43.60	5.47	0.28
Pt_3 - P	⑧	13.5	tectonic belt mélange strata	2.600	12.95	1.49	2.04	46.26	0.58	0.64
P	⑦	7.55	mudstone	2.603	9.10	0.70	0.82	38.13	0.70	0.18
	⑥	12.08	sandy mudstone	2.646	13.50	0.70	4.00	34.21	0.78	0.10
	⑤	21.13	siltstone	2.750	61.80	2.25	2.25	39.00	3.40	0.28
	④	15.40	fine sandstone	2.836	76.42	4.04	4.40	34.22	4.30	0.20
	③	14.04	mudstone	2.610	10.10	0.72	0.85	37.30	0.70	0.19
	②	10.11	sandy mudstone	2.650	14.12	0.74	4.12	35.30	0.78	0.15
	①	6.64	fine sandstone	2.840	78.50	4.13	4.45	34.80	4.50	0.26
	0	8	coal seam	1.400	13.50	0.55	0.04	20.20	0.001	0.27
	-1	10	mudstone	2.630	29.40	1.70	2.40	38.32	0.72	0.23

3.2 Numerical simulation

Given the geometric parameters of the 1307 FMTC working face and lithological features of surrounding rock mass, numerical simulation modelling on the precondition of large mining heights was built by coupling elastoplastic finite element model (FEM) in rock mechanics with "no-tension analysis" (NTA), or "FEM-NTA coupling". The model has a strike length of 1,500m and slope width of 200m, vertical height of 235.82m (including floor rock 10m, 13-1# coal seam 8m, roof rock 86.95m, mélange strata in tectonic belt 13.5m, and lower Proterozoic gneiss strata 118.37m). Over the lower Proterozoic gneiss strata are Quaternary strata 183.93m, the load of which is evenly distributed on the upper boundary of the model.

(1) Boundary conditions. In the model, the upper boundary is free boundary (i.e. unconstrained movement on x-axis and z-axis). Left and right boundaries are single-constrained boundaries (i.e. free movement on z-axis, constrained movement on x-axis). Lower boundary is fully constrained (i.e. constrained movement on both x-axis and z-axis).

(2) No-tension analysis. For ideal plastic model, Drucker-Prager yield criterion is most frequently used to determine whether a material has failed or undergone plastic yielding. However, the criterion has constraints in, on one hand, underestimating displacements and, on the other, overestimating tensile stress in the model to the point higher than the rock's tensile strength, which is unrealistic. In order to make to these constraints in Drucker-Prager criterion, this research treated the low tensile strength of rock mass as "no-tension".

Under large mining heights in FMTC (6-10m), the rock mass demonstrates even lower tensile strength. The way stress adjusts, transfer, or redistribute inside roof rock conforms to the conditions in no-tension analysis.

Rock discontinuities are not uncommon, which is why the rock has low resistance against tensile stress or even to none. Therefore, in elastic solution for rock mechanics, the super high tensile stress shown in some parts is in effect nonexistent. The argument is that if local tensile stress in rock mass surpasses its tensile strength, the local part is supposed to crack, thus bringing tensile stress to zero before the stress redistributes. While in this process, the same may happen to other parts of the rock mass, where the local tensile stress is bigger than tensile strength, and new crack causes internal tensile stress to redistribute [27]. As stress redistributes, there will be cracks in the rock mass. The tensile stresses which were larger than rock's tensile strength will be brought to zero due to the cracks. Other parts without cracks will be under compressive stress. In the end, there are two distinctive parts in the rock mass, one with cracks and one under compressive stress.

(3) Constitutive relation in tension failure. In the event of tensile stress in rock mass, the stress was not applied into Drucker-Prager yield criterion formula. Instead, it was compared with the rock's tensile strength. If tensile stress approaches tensile strength, the rule of tension failure was applied. In the case of tension failure, the cracked area could not bear the stress, which would readjust and redistribute.

To prove low tensile strength of roof rock under FMTC mining and large mining height, assume that the failure strain dε equals the sum of pre-failure linear strain dε_e^' and post-failure non-linear strain dε_p^', i.e. dε=dε_e^'+dε_p^'. As a result, the increments in main stress and main strain correlate as d{σ}=D_ep^t d{ε} (D_ep^t is the constant matrix of the material). The constitutive equation of tensile failure can be drawn in a similar way as in the elastic constitutive equation [28-29].

Before first failure:

$$f=\sigma_l-R_t\leq 0 \quad (1)$$

After first failure:

$$f=\sigma_l=0 \quad (2)$$

Where σ_l is main stress (l=1, 2)/Mpa and R_t is uniaxial tensile strength of rock mass/Mpa.

When σ_1≥R_t, failure condition is f=σ_1-R_t=0; when σ_1≥R_t, σ_2≥R_t, failure conditions are f_1=σ_1-R_t=0, f_2=σ_2-R_t=0.

(4) Simulation calculation. Using FEM-NTA coupled numerical simulation to simulate the movement and deformation of roof rock on No. 1307 FMTC working face in Xinji No. 1 Coalmine, assuming non-stop mining at an average height T=8m. Required physico-mechanical parameters of the coal seam and strata in roof and floor rock are available in Table 1.

In accordance with boundary conditions, principles of no-tension analysis, and constitutive relations of tension failure, the movement, deformation, and failure of roof bed can be simulated numerically. On dip section A-A' (see Figure 1), which is 50m away from the open-off cut, longitudinal stress distribution and roof rock failure are shown as in Figure 2 and Figure 3.

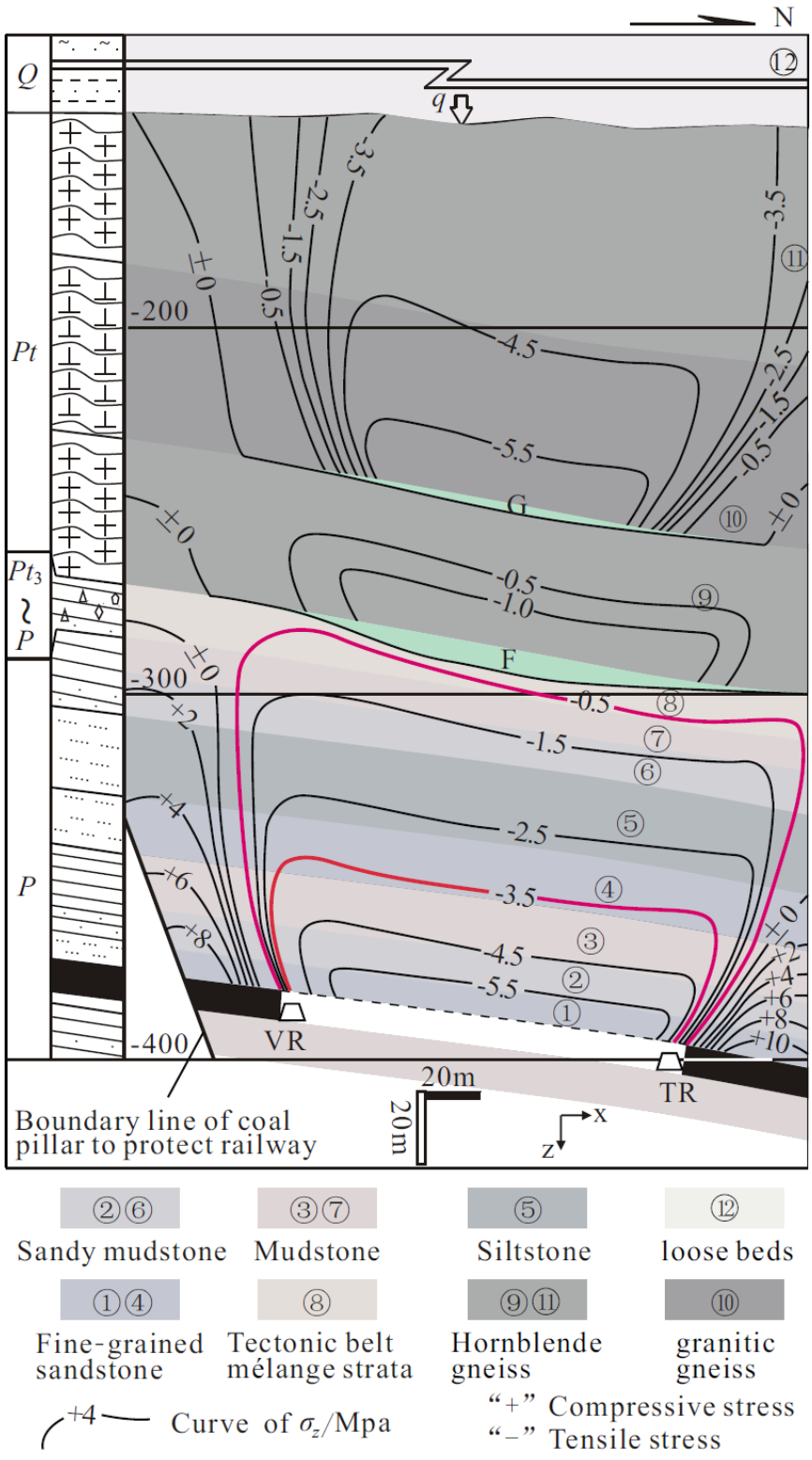

Figure 2. Longitudinal stress (σz) distribution in roof rock of No. 1307 FMTC working face (A-A' dip section)

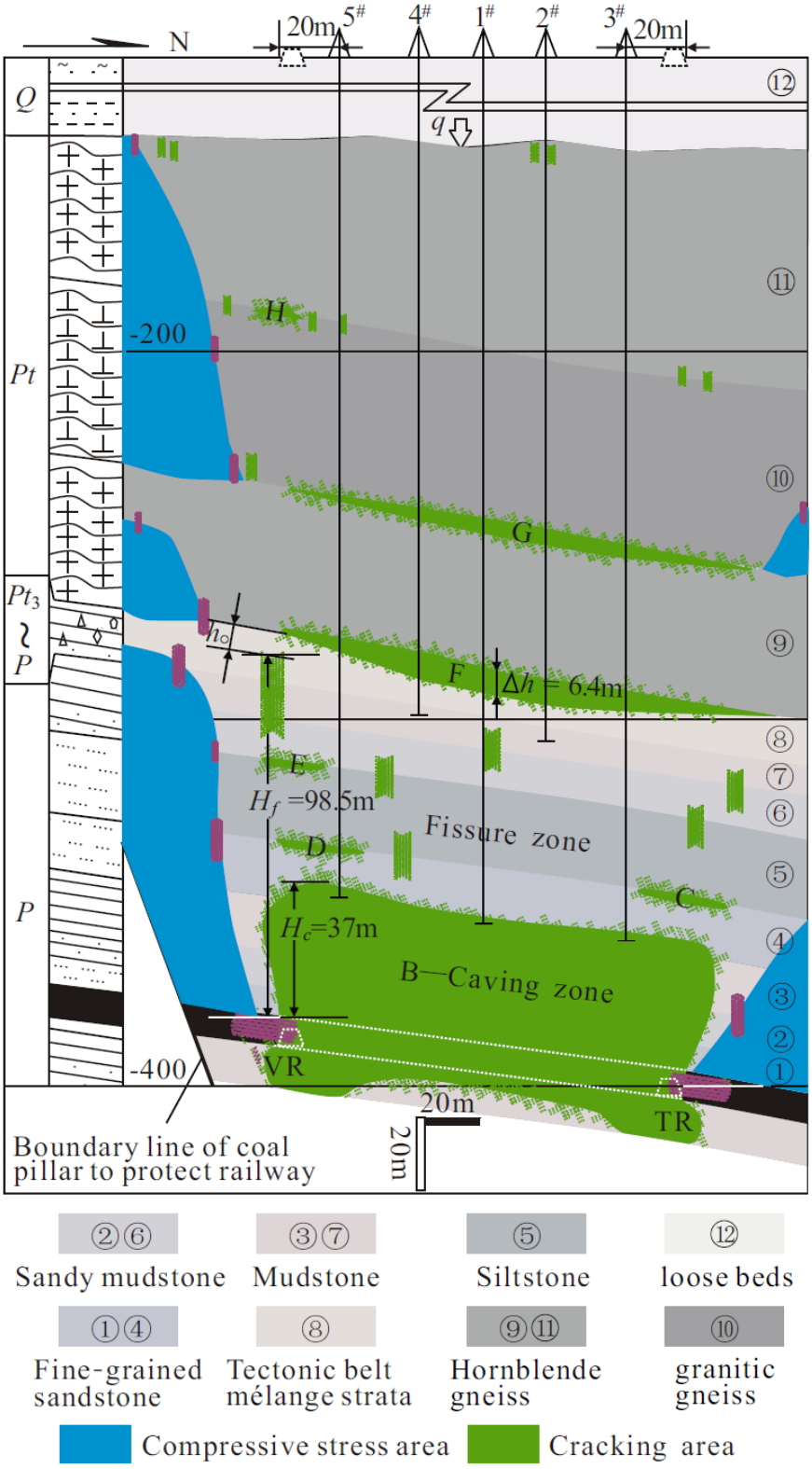

Figure 3. Deformation and failure characteristics of roof rock in No. 1307 FMTC working face (A-A' dip section)

3.3 Discussions

The following results can be obtained through FEM-NTA coupled numerical simulation in large mining height.

(1) Characteristics of failure zone. The longitudinal stress σz (as rock strata are near horizontal, σz is commensurate with the maximum principal stress σ1) has three isopleths of ±0 in the roof rock right above the goaf zone (Figure 2), which are corresponding to three marked failure zones (B, F, and G in Figure 3). Zone B is the closest to the goaf zone, where failure is the most severe and falls into the caving zone. Zone F and G shows discontinuum as stress transmits, indicating separation space. Additionally, smaller failure zones are identified in certain parts of the roof rock (C, D, E, and H in Figure 3), as well as a number of longitudinal tensile fractures.

(2) Heights of caving and fractured zone. In the roof rock beneath the bed separation F (Figure2), longitudinal tensile stress σz undulates regularly between -0.5Mpa to -5.5Mpa, which offers reference to map the water-conductive fractured zone and caving zone. (a) In Stratum ⑦ mudstone and Stratum ⑧ tectonic belt mélange strata, longitudinal tensile stress σz=-0.5Mpa to -1.5Mpa, close to the tensile strengths of the strata ⑦ (Rt=0.7Mpa) and ⑧ (Rt=1.49Mpa). This condition meets the mechanical criterion for tensile failure, thus the isopleth σz=-0.5Mpa is qualified as the outer curve of the water-conductive fractured zone in the roof rock. (b) Isopleth of longitudinal tensile stress σz=-4.5Mpa to -5.5Mpa spreads through Stratum ①fine sandstone (Rt=4.13Mpa), Stratum ② mudstone (Rt=0.74Mpa), and Stratum ③ sandy mudstone (Rt=0.72Mpa), where stress is far larger than the tensile strengths of each stratum. During mining, Strata ① to ③ are bound to collapse. In addition, though the isopleth of tensile stress σz=-3.5Mpa, which locates in the lower part of Stratum ④ fine sandstone, is slightly smaller than the stratum's tensile strength (Rt=4.04Mpa), the failure of Strata ① to ③ creates the mechanical conditions for local failure in Stratum ④. Therefore, isopleth σz=-3.5Mpa is ascertained as the outer curve of the roof caving zone.

With the outer curves of the water-conductive fractured zone (σz=-0.5Mpa) and the roof caving zone (σz=-3.5Mpa) in Figure 2 and the failure zone in Figure 3, converting by the vertical scale, the maximum heights of water-conductive fractured zone (Hf) and of caving zone (Hc) are respectively 98.5m and 37m (Figure 3). The ratio of Hf to the mining height (Hf /T) is 12.313, while Hc to the mining height (Hc /T) is 4.625 (T as mining height at 8m).

(3) Features of Zone G and F as bed separations. Figure 3 shows that G and F and the primary bed separations in the roof rock. In bed separation G, the upper strata are lower Proterozoic granitic gneiss in Stratum ⑩. Isopleth of longitudinal tensile stress σz=-5.5Mpa crosses through Zone G, 1.63 times the tensile strength of the strata (Rt=3.38Mpa). The upper Stratum ⑩ is, therefore, prone to rupture and the bed separation can exist for very short period. In bed separation F, the upper strata (Stratum ⑨) are lower Proterozoic hornblende gneiss. Isopleth of longitudinal tensile stress σz=-1.0Mpa crosses through Zone F, smaller than the tensile strength of the strata (Rt=1.52Mpa). Consequently, the bed separation can exist for longer period as the upper strata (Stratum ⑨) is suspended by larger space.

Bed separation G is away from the caving and fractured zone, having negligible influence on mining safety. By contrast, bed separation F is close to the caving and fractured zone with two sources of water: one as the underground water in the nappe structure and the other from the aquifer at the bottom of overlying Quaternary loose bed (the water in which flows in through the nappe tectonic belt or mining fractures). Therefore, water in bed separation F is a much bigger threat to production safety.

(4) Maximum width of bed separation F (∆h). Converting by the vertical scale, the maximum width of bed separation F, ∆h=6.40m (vertical), is located close to the center line of the goaf zone (Figure 3).

(5) Thickness of cushion layer (ho). Cushion layer refers to the strata between the bottom boundary of the bed separation and the ceiling boundary of the water-conductive fractured zone. Thickness of

such strata, at the maximum water-conductive fractured zone (Figure 3), is calculated as ho=（100.45-98.5）×cos8°=1.93m

(6) Verification by exploration. The cushion layer underlying bed separation F, thick as minimal as 1.93m (h0) tend to be torn broken under the pressure exerted by the weight of overlying rock and coalmine pressure. Under the high pressure, water confined in the bed separation would burst into working face through caving zone and fractured zone, endangering safety and productivity. The No. 1307 FMTC working face had suffered a number of bed separation water burst, the maximum water flow as high as 400m3/h, jolting production to a complete halt and incurring huge economic losses.

To verify the above analytical results using FEM-NTA coupled numerical simulation, five boreholes were drilled correspondingly at ground surface in the 1307 FMTC working face (Figure 3: borehole 1#, 2#, 3#, 4# and 5#), of which drill 1# was in the center of goaf zone (Figure 3). Drills into F, G, and H, which are bed separations, consumed much more washing fluid. Drill 1#, past through the bottom of Stratum ⑨, slipped and the drill core broken. Imaging of drill 3# and 5# showed a residual separation, height of 0.54m, at the bottom of Stratum ⑨ hornblende gneiss. Exploratory observations confirmed the viability of the coupled numerical simulation introduced in this article.

4. Conclusions

Following conclusions are drawn based on the analysis above:

- Fractures developing in rock mass compromises the rock's tensile stress. The larger the mining height, the weaker the roof rock's strength against tensile stress. Therefore, to conform to the low tensile strength, this article introduces a method to simulate the deformation of roof rock under large mining height by coupling elastoplastic finite element model (FEM) in rock mechanics with "no-tension analysis" (NTA).
- The No. 1307 FMTC working face of Xinji No. 1 Coalmine, Anhui Huainan Mining Field in North China coal-bearing region, was selected as the research target. The research started by taking rock and coal samples through drilling, which were then processed to determine the physico-mechanical properties of the nappe structure and coal measures. The data were then applied into FEM-NTA coupled numerical simulation to model the stress distribution and deformation characteristics of rook rock when mining thick coal seam under nappe structure, with quantitative results of the location and widths of caving zone, water-conductive fractured zone, and bed separation zone.
- Analysis of the quantitative results showed that between the two main bed separations (G and F), G is farther away from the water-conductive fractured zone. The strata (Stratum ⑩) over G are more likely to rupture due to larger load of tensile stress. In the event of rupture, the separation would be closed up and neutralize the threat to mining safety. However, bed separation F is closer to the water-conductive fractured zone by only 1.93m. The strata (Stratum ⑨) over F, bearing a tensile stress commensurate with its tensile strength, were suspended for longer period and crated larger separation space (maximum at 6.4m), thus posing a bigger threat to mining safety.

Acknowledgment(s)

This article is funded by National Natural Science Foundation of China (41773100, 41373095), Practical and Innovative Project of Coal Geology Bureau of Shanxi Province (2017) and Research Project of Wanbei Coal-Electricity Group Co. Ltd (2018).

References

[1] T.J. Fan. A comprehensive guidebook to water control in coalmines.Jilin Audio-Visual Press, Jilin: Changchun, pp.3-31, 2003.
[2] H.R. Gui, M.L. Lin. Types of water hazards in China coalmines and regional characteristics. Natural Hazards, Vol.84, no.2, pp.1501-1512, 2016.
[3] T. Majcherczyk, P. Małkowski, Z. Niedbalski. Rock mass movements around development

workings in various density of standing-and-roof-bolting support. Journal of Coal Science & Engineering(China), Vol.14, no.3, pp.356-360, 2008.
[4] J.L. Xu, M.G. Qian, H.W. Jin. Study and application of bed separation distribution and development in the process of strata movement. Chinese Journal of Geotechnical Engineering, Vol.24, no.5, pp.632-636, 2004.
[5] W.P. Li, X.Q. Li, R.H. Sun. Preliminary study on dynamic water Inrush of coal mining under super-thick dead Rock. Journal of Engineering Geology, Vol.16, no.(S1) pp.446-450, 2008.
[6] W.J. Guo, Y.Y. Li, D.W. Yin, S.C. Zhang, X.Z. Sun. Mechanisms of rock burst in hard and thick upper strata and rock-burst controlling technology. Arabian Journal of Geosciences, Vol.9, no.10, pp.561, 2016.
[7] H.R. Gui, M.L. Lin, X.M. Song, Features of separation water hazard in China coalmines. Water Practice & Technology, Vol.12, no.1, pp.146-155, 2017.
[8] W. Qiao, W.P. Li, R.H. Sun, X.Q. Li, G. Hu. Formation mechanism of dynamic impact failure zone of super dynamic water inrush in coal mine. Chinese Journal of Geotechnical Engineering, Vol. 33, no.11, pp. 1726–1 733, 2011.
[9] T.B. Zhao, Y.C. Yin, Y.L. Tan. Safe mining and new prediction model in coal seam with rock burst Induced by roof. Disaster Advances, vol.5, no.4, pp.961-965, 2012.
[10] D. Z hang, J.C. Wang, P.S. Zhang, B. Shi. Internal strain monitoring for coal mining similarity model based on distributed fiber optical sensing. Measurement, no.97, pp.234-241, 2017.
[11] Y.L. Tan, F.H. Yu, L. Chen. A new approach for predicting bedding separation of roof strata in underground coalmines. International Journal of Rock Mechanics & Mining Sciences, no.61, pp.183-188, 2013.
[12] B.K. Hebblewhite, T. Lu. Geomechanical behaviour of laminated, weak coal mine roof strata and the implications for a ground reinforcement strategy. International Journal of Rock Mechanics & Mining Sciences, vol.41, no.1 ,pp.147-157, 2004.
[13] A.N. Jemcik, B. Indraratna, W. Gale. Floor failure analysis at a longwall mining face based on the multiple sliding block model. Geotechnical & Geological Engineering vol.18, no.3, pp.175–192, 2000.
[14] S.T. Kuznetsov, B.Z. Amusin, D.G. Pekarskii. Approximate calculation of the risk of bed separation in coal seam roofs. Soviet Mining Science, vol.12, no.4, pp.359-364, 1976.
[15] S.T. Kuznetsov, N.A. Filatov, N.F. Dontsul. Predicting bed separation in roof rocks of rooms. Soviet mining science, vol.16, no.4, pp.316-319, 1980.
[16] M.G. Qian, X.X. Miao, J.L. Xu. Theoretical study of key stratum in ground control. Journal of China Coal Society, vol.21, no.3, pp.225-230, 1996.
[17] X.X. Miao, X.B. Mao, Z.W. Sun, H. Pu. Formation conditions of compound key strata in mining overlayer strata and its discriminance. Journal of China University of Mining & Technology, vol.34, no.5, pp.547-550, 2005.
[18] J.L. Xu, X..Z Wang, W.T. Liu, Z.G. Wang. Effects of primary key stratum location on height of water flowing fracture zone. Chinese Journal of Rock Mechanics and Engineering, vol.28, no.2, pp.380-386, 2009.
[19] J.Q. Zhang, G.H. Liao. Study of the mechanism and the calculation methods about bed separation in overlying strata. Underground Space, vol.21, no.5, pp.407-411,417, 2001.
[20] D.S. Zhao, G.Y. Zhu, W.S. Liu, X.L. Fan. Test study on the laws of overburden separation layer. Journal of Liaoning Technical University (Natural Science), vol.21, no.1, pp.4-7, 2002.
[21] L. Yang, G.M. Yu, X.C. Wang, R. Tian, L.H. Li. Calculation of position of separated strata due to mining in coal mine. Journal of China Coal Society, vol.22, no.5, pp.477-480, 1997.
[22] S.R. Wang, N. Li, C.L. Li, C. Cao. Distribution characteristics analysis of pressure-arch in horizontal stratified rocks under coal mining conditions. Tehnicki Vjesnik-Technical Gazette, vol.22, no.4, pp.997-1004, 2015.
[23] A.K. Verma, D. Deb. Effect of lithological variations of mine roof on chock shield support

using numerical modeling technique. Journal of Scientific & Industrial Research, vol.65, no.9, pp.702-712, 2006.

[24] H. Yan, J.X. Zhang, Z.W. Ding, Y.L. Huang. Surrounding rock deformation mechanism of roadways with extra-thick coal seam. Disaster Advances, vol.6, no. S6, pp.226-233, 2013.

[25] H. Yan, X.J. Deng, K. Fang , S. Guo, W.K. Li. Roof catastrophe mechanism of roadways with extra-thick coal seam and its controlling countermeasures. Disaster Advances, vol.6, no.5, pp236-243, 2013.

[26] Z.J. Su, G.M. Yu, L. Yang. Numerical simulation on mechanism of deformation of separated strata in overburden. Chinese Journal of Rock Mechanics and Engineering, vol.22, no.8, pp.1287-1290, 2003.

[27] D.S. Zhao, X. Chen, L.K. Jia, T. Xu, P. Guan. Numerical simulation on mining induced bed separation of overlying strata. Chinese Journal of Rock Mechanics and Engineering, vol.24, no.S1, pp.5164-5167, 2005.

[28] H.R. Gui, Q.F. Zhou, D.X. Liao, Q.E. Kang, Z.Y. Fan. Prediction of maximum height of the fractured zone by stressing method for sub-level caving mining. Journal of China Coal Society, vol.22, no.4, pp.375-379, 1997.

[29] H.R. Gui, L.W. Chen, X.M. Song, M. Tu, Y. Qin. Research on water and sand control for coalmining in the shallow part of areas covered by thick loose-bed.China University of Mining and Technology Press, Jiangsu: Xuzhou, pp.210-252, 2015.